

Article

# Mineralogical and Environmental Geochemistry of Coal Combustion Products from Shenhua and Yihua Power Plants in Xinjiang Autonomous Region, Northwest China

Peng Wu <sup>1</sup>, Jing Li <sup>1,\*</sup>, Xinguo Zhuang <sup>1</sup>, Xavier Querol <sup>2</sup>, Natalia Moreno <sup>2</sup>, Baoqing Li <sup>1</sup>, Dongfeng Ge <sup>3</sup>, Shihua Zhao <sup>4</sup>, Xiaoping Ma <sup>3</sup>, Patricia Cordoba <sup>2</sup> and Yunfei Shangguan <sup>1</sup>

<sup>1</sup> Key Laboratory of Tectonics and Petroleum, Ministry of Education, China University of Geosciences (Wuhan), Wuhan 430074, China

<sup>2</sup> Institute of Environmental Assessment and Water Research, CSIC, C/Jordi Girona 18-26, 08034 Barcelona, Spain

<sup>3</sup> Xinjiang Bureau of Prospecting and Development of Geology and Mineral Resources, Urumqi 830000, China

<sup>4</sup> The Fifth Prospecting Team of Shandong Coal Geology Bureau, Tai'an 271000, China

\* Correspondence: jingli@cug.edu.cn; Tel.: +86-1369-734-8536

Received: 2 July 2019; Accepted: 16 August 2019; Published: 19 August 2019



**Abstract:** The mineralogical and geochemical characteristics of feed coals and coal combustion products (CCPs) from the Shenhua and Yihua Power Plants in Xinjiang Autonomous Region, were studied by means of proximate analysis, Power X-ray diffraction (XRD), scanning electron microscopy with Energy Dispersive X-ray analyzer (SEM-EDX), inductively coupled plasma atomic emission spectrometry (ICP-MS) and inductively coupled plasma mass spectrometry (ICP-AES). The environmental geochemistry of CCPs was evaluated by Al-normalized enrichment factor as well as European Standard EN-12457 leaching test. Two feed coals have the characteristics of low sulfur content, medium to high volatiles matter yields, medium moisture content, super low to medium ash yield, medium to high calorific value and low mineral content. The main crystalline facies in fly ash and slag are quartz and mullite, with a small amount of calcite, and some unburned carbon. Hematite, SrSO<sub>4</sub> and barite also can be observed in fly ashes by SEM. Typical plerophere occurs in fine fly ash rather than the coarse fly ash. The concentration of most trace elements in CCPs falls within the lower concentration range of European fly ashes. With respect to the partitioning behavior of trace elements during coal combustion, S is highly volatile, and Mg, Na, Zn, B, Co, As, Nb, Zr, Cu and K also show certain volatility, which may to some extent emit to the atmosphere. Furthermore, leaching experiments show that leachable concentrations of most of the potentially toxic elements in CCPs are low, and the CCPs fall in the range between inert and nonhazardous landfill material regulated by the 2003/33/EC Decision.

**Keywords:** coal combustion products; mineralogy; environmental geochemistry; partitioning behavior; leachability; Shenhua power plant; Yihua power plant

## 1. Introduction

China is the largest producer and consumer of coal in the world [1], which relies on coal for 70% of its energy needs. In 2018, coal consumption reached 2.7 billion tons [2], or about 1.9 billion tons of oil equivalent (1 ton of oil is equivalent to 1.43 tons of standard coal), accounting for 50.58% of global coal consumption. According to the China's 13th five-year plan (2016–2020) for National Economic and Social Development, China plans to cap coal consumption at 4.1 billion tons by 2020 [3],

which implies coal consumption will rise sequentially [4–6]. The use of coal resources promotes economic development, meanwhile, air pollutants, particulate matter, as well as CCPs from coal combustion cause serious environmental problems [7–10].

With increasing environmental concerns, the need for research on potential applications for CCPs has become more environmentally relevant [11]. Nowadays, a large proportion of CCPs has been used for different purposes worldwide [9,12–14]. However, large volumes of the world's CCPs, especially unexploited fly ashes are still discharged into ash ponds, landfills, and/or lagoons [15–17]. The CCPs may contain relatively high concentrations of elements of environmental concern. A number of these elements may be present in highly leachable species, increasing their potential environmental and health impacts, especially when large amounts of CCPs are disposed of in lagoons and landfills. Furthermore, the emplacement of CCPs also involves significant costs and environmental impacts associated with landfill disposal [9]. On the other hand, the high volume of coal usage in China has increasingly focused attention on the valuable elements that may occur in the coal and associated ash (e.g., Ge, Ga, U, rare earth elements and Y, Nb, Zr, Se, V, Re, Au, and Ag, as well as the base metal Al) [1]. Coal and coal ash can also be considered as an economic source of strategically important valuable elements, when these elements in several coals (or coal ashes) and some coal-bearing strata occur at concentrations comparable to or even higher than those in conventional economic deposits [18–20]. For instance, two Chinese (Lincang and Wulantuga) and one Russian (Spetzugli, Pavlovsk Coalfield) Ge-bearing coal deposits are currently being mined where Ge is recovered from the fly ash, with the Ge production from these deposits accounting for more than 50% of the total industrial Ge production in the world [21,22]. Laudal et al. (2018) study suggests that rare earth elements can be extracted from lignite by acidic solution [23]; Zhang et al. (2018) found that rare earth elements recovery use staged precipitation from a leachate generated from coarse coal refuse [24]. In addition, CCPs might also be utilized as other recoverable resources for various applications depending on the manifold physico-chemical characteristics of CCPs, for instance, synthesis of zeolite, geopolymer, recovery of cenospheres, and so on [9,25,26]. As a consequence, investigations into the various characteristics of CCPs are environmentally beneficial and of high economic and social significance from the viewpoint of both CCP disposal and CCP utilization.

There are enormous coal resources from several large coal basins, with various coal characteristics in Xinjiang, and a number of studies have been extensively carried out on the Xinjiang coals and coal ashes [27–29]. Dai et al. (2015) reported that the Yili coals are characterized by high concentrations of U (up to 7207 µg/g), Se (up to 253 µg/g), Mo (1248 µg/g), and Re (up to 34 µg/g), as well as As (up to 234 µg/g) and Hg (up to 3858 ng/g), and industrial materials can be extracted from it [29]. The super-large eastern Junggar coals are of high quality with low trace element concentrations except Na, Sr, and Ba [25,26]. The Xinjiang lignite mined from Shaerhu coalfield (SEHc) easily causes severe fouling and corrosion because of its high sodium and chlorine contents [30]. Zhang et al. (2018) adopted sequential chemical extraction experiment (SCEE) to quantitatively determine the arsenic occurrence modes of high-arsenic coal from Hanshuiquan district, Santanghu Coalfield [31]. Furthermore, previous studies have also been made on the structural properties of coal and the variation of ash content of coal ash in Xinjiang [32–34]. The environmental characteristics of CCPs, especially the leaching and partitioning behavior, are extremely important properties that influence their further disposals and applications. The Leaching Environment Assessment Framework (LEAF) proposed by the United States Environmental Protection Agency was adopted by Zhang et al. (2019), discussing the modes of occurrence and causes of mobility of trace elements in CCPs [35]. Yang et al. (2019) investigate leachate and mobility of elements in uranium-enriched coal ash with thermo chemical treatment [36]. Li et al. (2012) reported that CCPs from two power plants in Xinjiang has low environmental threat, which is beneficial to the subsequent application [37]. Nevertheless, given the aforementioned various characteristics of coals in Xinjiang, the CCPs generated are supposed to have diverse characteristics with different environmental implications. Therefore, the significance of research on various characteristics of CCPs in Xinjiang cannot be overemphasized. Due to the increasing energy demand in China and

large clean coal resources in Xinjiang, especially in Junggar coal field, recently, there are many coal-fired power plants near the Junggar coalfield, which produce a large amount of CCPs. The present study aims at investigating the mineralogical and environmental geochemistry of feed coals and CCPs from the Shenhua and Yihua power plants, located in eastern Junggar coalfield, with emphasis on the study of trace elements, especially their leaching potential and partitioning behavior during combustion, in order to assess their environmental impacts and potential for further application [35,36,38].

## 2. Samples and Methods

### 2.1. Sampling and Power Plant Description

Sampling was carried out at two pulverized coal combustion (PCC) power plants in Xinjiang Province, viz., the Shenhua and Yihua power plants (Figure 1). The Shenhua and Yihua power plants are located in the Wucaiwan mining area, eastern Junggar coalfield. It is very convenient for the feed coal transportation due to superior geographical position.

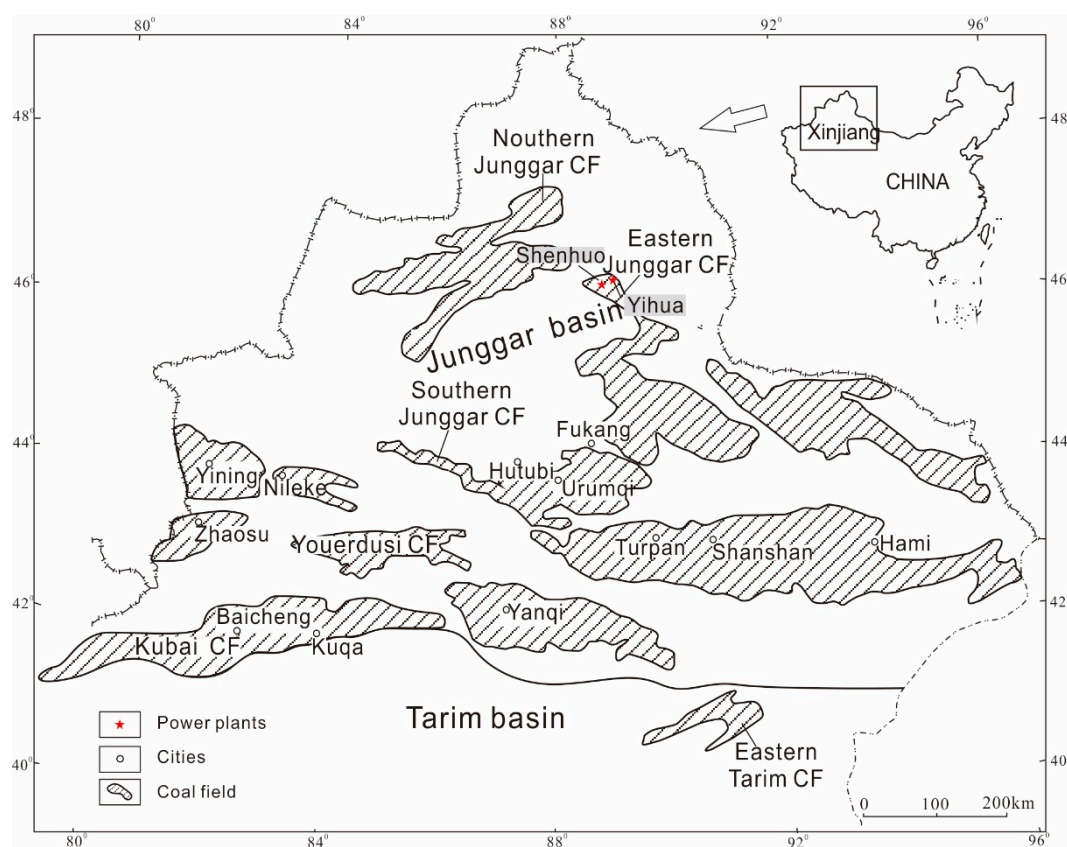


**Figure 1.** Location of Shenhua and Yihua power plants (modified after Li et al., 2012) [37].

The Shenhua power plant, supporting construction of  $4 \times 350$  MW power station project, utilizing domestic supercritical indirect air-cooled coal-fired thermal power generation units, with a total installed capacity of 1400 MW, consumes 15,000–16,000 tons of feed coal per day. The Yihua power plant assembles  $2 \times 330$  MW power station project and consumes 6000 tons of feed coal per day.

The operating conditions of both plants are characterized by pulverized-coal (PC) boilers, electrostatic precipitators (ESP) and a limestone-gypsum wet flue gas desulfurization system (WFGD). The two power plants are both fed with a blend of coals from different coal fields in Xinjiang but mainly from the Junggar coal basin.

The feed coal, fly ash, and slag samples were simultaneously collected at the Shenhua and Yihua PCC power plants in July 2017. One feed coal (S-C), one slag (S-Slag), and two fly ash samples

(one coarse and one fine fraction from different rows of the electrostatic precipitators (ESP), S-FAf, S-FAc, respectively) were taken from the Shenhua power plant. One feed coal (Y-C) one fly ash (Y-FA) and one slag (Y-Slag) sample were collected from the Yihua PCC plant.

The fly ash/slag ratio was 9:1 (90% and 10% of the production, respectively) at both Shenhua and Yihua power plants. Furthermore, the production of fine and coarse fractions of fly ash in the Shenhua power plant with a 2:3 fine/coarse fly ash ratio should be noted.

Around 1kg of each sample were collected, split, and 50 g of each sample were crushed and milled to different grain size for subsequent analyses.

## 2.2. Methods

Proximate analysis of feed coal was performed following ASTM-Standards D3173-11, D3174-12 (2018), and D3175-18 [39–41]. Elemental analysis (N, C, S, H) of feed coal, fly ash, and slag were determined by an Element instrument (Vario EL III, Elementar Trading (shanghai), Shanghai, China). Grain size distribution of CCPs was analyzed by Mastersizer2000 (Malvern Instruments, Worcestershire, UK). The mineralogical composition was analyzed by XRD and SEM-EDX. When applying XRD map scanning, the interval of 2 theta is 2.6–70°, and step length is 0.01°. Semiquantitative XRD analysis was performed by using the matrix flushing method devised by Chung (1974) and calculating the integrated area of the main peak for the different mineral phases in each sample [42]. Fluorite (CaF<sub>2</sub>) in binary mixtures was used as an internal standard to determine the diffraction constants against fluorite for each mineral phase [43]. This method is based on the XRD intensity ratio between a crystalline phase and an internal standard. This method first requires the calculation of the XRD constants for each crystalline phase by applying the Klug and Alexander equation [44]. Subsequently, the material under study is spiked with the internal standard and analyzed by XRD to obtain the proportions of each crystalline phase of the sample. The microstructure of minerals and morphology of CCPs were observed by QUANTA840 SEM-EDX (FEI, Hillsboro, OR, USA).

Feed coal, fly ash, and slag samples were acid-digested by using a two-step digestion method devised by Querol et al. [45]. The resulting solutions were then analyzed by Inductively-Coupled Plasma Atomic-Emission Spectrometry (ICP-AES) (Iris Advantage TJA Solutions, Thermo Fisher Scientific, MA, USA) for major and selected trace elements (Ti, Mn, P, B, Ba, Cu, Ni, Sr, Zn and V), and by Inductively-Coupled Plasma Mass Spectrometry (ICP-MS) (X-Series II Thermo, Thermo Fisher Scientific, Waltham, MA, USA) for most trace elements. Logically the content of above trace elements must be higher than the detection limit of ICP-AES. We do it as an intra-comparison exercise, which is a way to compare both results and know if the determination results are precise.

As aforementioned, extensive studies have been carried out on leaching of coal combustion by-products [35,36,38]. In this paper, the European Standard leaching test EN-12457 [46] was applied to fly ash and slag samples to evaluate the leaching potential of major and trace elements. The standard EN 12457 batch leaching test (Liquid/Solid ratio of 10 L per kg in MilliQ water which were produced by Mill-Q ultrapure water preparation system), 24 h agitation at ambient temperature) was undertaken on the CCP samples to study the solubility and mobility of trace elements from the CCPs. Thereafter, the solution was filtered, respectively, and the leachable concentrations of major and trace elements in the extracts were measured by ICP-AES and ICP-MS.

## 2.3. Data Treatment

In order to measure the distribution of elements in flue gas, fly ash and slag during coal burning in Shenhua and Yihua power plant, Al is considered as a non-volatile element, and aluminum normalization enrichment factor, is used to quantify the enrichment of the major and trace elements in fly ash (EF<sub>A</sub>) and slag (EF<sub>S</sub>) [37,47,48]. Meanwhile, normalized (fly ash + slag)/feed coal enrichment factors (total enrichment factors, EF<sub>T</sub>) is calculated by the following formula:  $EF_T = EF_A \times A + EF_S \times B$ , where A and B are the production proportion of the fly ash and slag (90% and 10% respectively)

When the enrichment coefficient  $EF_A$  or  $EF_S > 1$ , it indicates that the element is enriched in fly ash or slag. The enrichment coefficients of low volatile elements are  $\approx 1$ , those of high volatile elements are  $< 1$ .  $EF_T$  can indirectly determine the volatility of each element in feed coal. Thus,  $EF_A < 1$ ,  $EF_S < 1$  or  $EF_T < 0.9$  indicate that the elements in the feed coal volatilize (the error of this method is about 10–15%).

### 3. Results and Discussion

#### 3.1. Feed Coal Characteristics

Eastern Junggar coal is high volatile bituminous, with vitrinite reflectance of 0.40–0.50%. As shown in Table 1, the feed coals of Shenhua and Yihua power plants show the characteristics of low sulfur content, super low to high volatile matter yield, medium moisture content, low-medium ash yield and medium-high calorific value. The feed coals belong to medium-high volatile bituminous, which is basically in line with previous studies [49].

**Table 1.** Proximate analyses of feed coals from Shenhua and Yihua power plants. Y-C, feed coal from Yihua power plant; S-C, feed coal from Shenhua power plant; ad—air dry basis; db—dry basis; daf—dry, ash-free; ar—as received basis; HTA—high temperature ash, VM—volatile matter; CV—calorific value.

Feed Coal	M (ad, %)	HTA (d, %)	VM (daf, %)	C (daf, %)	S (db, %)	CV(ar, MJ/kg)
Y-C	12.32	4.81	31.97	68.03	0.52	22.22
S-C	11.33	13.86	34.68	65.32	0.50	23.36

Quartz ( $\text{SiO}_2$ ) and Kaolinite ( $\text{Al}_4[\text{Si}_4\text{O}_{10}](\text{OH})_2$ ) are the major minerals occurring in two feed coals. In addition, traces of gypsum ( $\text{CaSO}_4 \cdot 2\text{H}_2\text{O}$ ) and calcite ( $\text{CaCO}_3$ ) were also detected in S-C. In general, the total mineral content of feed coals is low, among which the content of clay minerals and quartz is relatively high, while that of pyrite is lower, due to the continental sedimentary coal-forming environment.

The concentrations of major and trace elements in feed coals are listed in Table 2. Compared with the average content of major elements in Chinese coals [50], calcium and sodium are slightly higher, while the depletion of aluminum, iron, and titanium is obvious, and the content of, magnesium and potassium is close to the average (Table 2).

As described in the Table 2, the concentrations of trace elements in feed coals are compared with the average for China coals reported by Dai et al. (2012) and world low-rank coals reported by Ketriss and Yudovich (2009) [26,51]. According to the concentration coefficients normalized to average trace element concentration for Chinese and worldwide coals [29], except Sr and Ba in S-C, the contents of most elements in two feed coals fall in the lower range of the worldwide concentration ranges, and lower than the average values of worldwide coals [51]. Analogously, when compared with the content in Chinese coals, only Sr and Ba in S-C are higher than the average value, and content of other elements are low (Figures 2 and 3). In summary, except for Sr and Ba in S-C, the content of other trace elements in feed coals, including those closely related to the environment, e.g., As, Hg, Be, Cr, Co, Ni, Cu, Zn, Se, Mo, Cd, Sn, Sb, Pb, Bi is relatively low. The higher Sr and Ba content in feed coal is consistent with those in eastern Junggar coals [26]. Consequently, the feed coal of Shenhua and Yihua power plants, from the perspective of environmental protection, possesses high quality.

**Table 2.** Major oxide content (%) and trace element concentrations (mg/kg) of feed coals and corresponding values in Chinese and Worldwide coal. Y-C, feed coal from Yihua power plant; S-C, feed coal from Shenhua power plant.

	Y-C	S-C	Chinese <sup>a</sup>	World <sup>b</sup>		Y-C	S-C	Chinese <sup>a</sup>	World <sup>b</sup>
%					mg/kg				
Al <sub>2</sub> O <sub>3</sub>	0.9	2.9	6	nd	As	1.1	4	3.8	8.3
CaO	1.3	1.6	1.2	nd	Se	<dl	<dl	2.5	1.3
Fe <sub>2</sub> O <sub>3</sub>	0.2	0.9	4.9	nd	Rb	2.2	4.4	9.3	14
K <sub>2</sub> O	0.1	0.1	0.2	nd	Sr	165	314	140	110
MgO	0.3	0.3	0.2	nd	Y	1.5	4.6	18	8.4
Na <sub>2</sub> O	0.3	0.2	0.2	nd	Zr	8.7	33.4	90	36
SO <sub>3</sub>	0.5	1.3	0.25	nd	Nb	<dl	1.6	9.4	3.7
mg/kg					Mo	<dl	<dl	3.1	2.2
Li	2.1	4.5	32	12	Cd	<dl	<dl	0.3	0.2
Be	<dl	<dl	2.1	1.6	Sn	<dl	<dl	2.1	1.1
B	52.5	47.1	53	52	Sb	<dl	<dl	0.8	0.9
P	38.5	314.3	402	nd	Cs	<dl	<dl	1.1	1
Sc	<dl	<dl	4.4	3.9	Ba	34.3	335	159	150
Ti	246	723	1980	nd	La	1.7	6.4	22.5	11
V	5.0	22.5	35	25	Ce	3.1	11.7	46.7	23
Cr	3.5	9.9	15	16	Sm	<dl	1.2	4.1	2
Mn	27.1	124	116	nd	Dy	<dl	0.8	3.7	2.1
Co	3.8	3.6	7.1	5.1	Hf	<dl	<dl	3.7	1.2
Ni	5.0	6.6	14	13	W	<dl	<dl	1.1	1.1
Cu	2.0	17.3	18	16	Pb	0.8	3.8	15.1	7.8
Zn	14.2	16.5	41	23	Th	<dl	1.8	5.8	3.3
Ga	<dl	2.6	6.6	5.8	U	<dl	<dl	2.4	2.4
Ge	<dl	<dl	2.8	2.2					

<dl: under detected limit; nd: no data; a Data from [50]; b Data from [51].

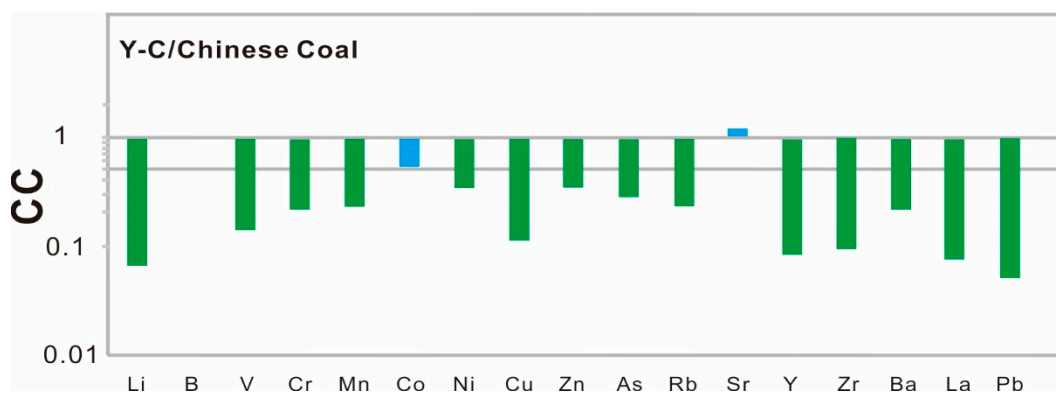
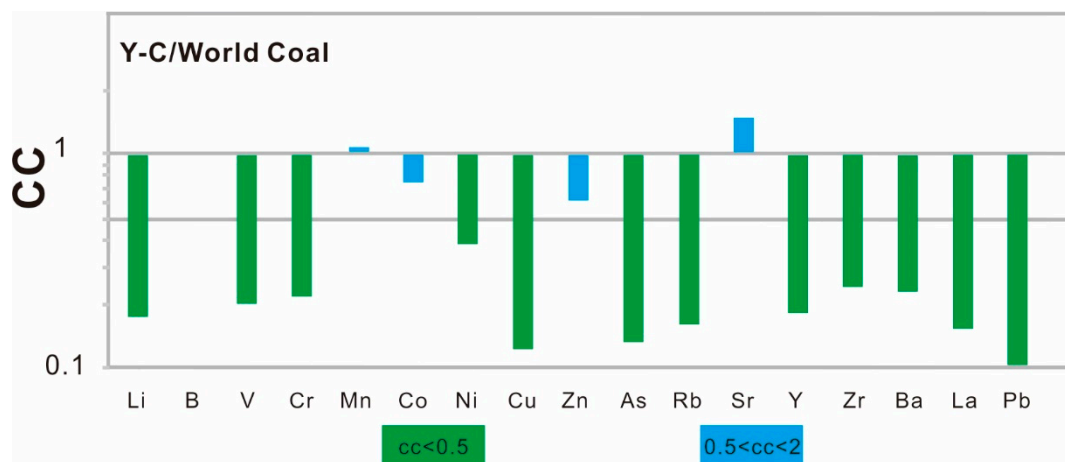
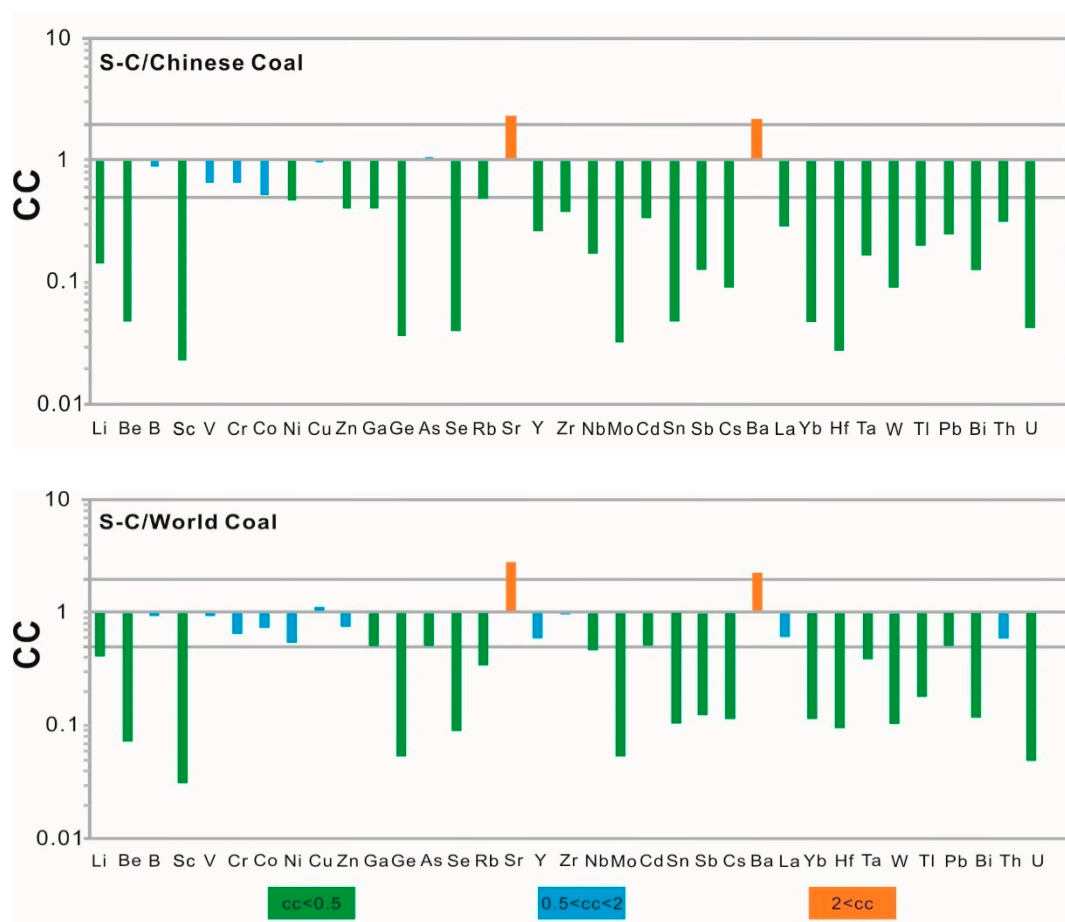


Figure 2. Cont.



**Figure 2.** Concentration coefficients of trace elements in feed coal from Yihua power plant normalized to average values in Chinese [50] and worldwide [51] coals (modified after Dai et al., 2015) [29].



**Figure 3.** Concentration coefficients of trace elements in feed coal from Shenhua power plant normalized to corresponding average values in Chinese [50] and worldwide [51] coals (modified after Dai et al., 2015) [29].

### 3.2. Fly Ash and Slag Characterization

#### 3.2.1. Physical Characteristics

As shown in Figure 4, through Mastersizer2000 particle size analysis, it is obvious that the particle size of S-FAc is smaller than that of S-FAc. S-FAc is characterized by a trimodal lognormal grain size

distribution with a prevalent coarse mode over two fine mode (Figure 4). The particle size of S-FAc is concentrated around 150  $\mu\text{m}$ , which is between 0.4 and 503  $\mu\text{m}$ , with P10 (10th percentile) of 2.58  $\mu\text{m}$ , P50 of 64.84  $\mu\text{m}$  and P90 of 239.05  $\mu\text{m}$ . By contrast, S-FAf shows a bimodal grain size distribution, with one peak of around 5  $\mu\text{m}$  and the other of 60  $\mu\text{m}$ . The particle size of S-FAf is between 0.4 and 282  $\mu\text{m}$ , with P10 of 1.96  $\mu\text{m}$ , P50 of 14.41  $\mu\text{m}$  and P90 of 98.47  $\mu\text{m}$ . The characteristics of Y-FA is similar to S-FAf, with one peak of around 3  $\mu\text{m}$  and the other of 40  $\mu\text{m}$ . The particle size of Y-FA is between 0.4 and 224  $\mu\text{m}$ , with P10 of 1.23  $\mu\text{m}$ , P50 of 8.03  $\mu\text{m}$  and P90 of 67.18  $\mu\text{m}$ , suggesting that the particle size of Y-FA is the tiniest among the three fly ashes.

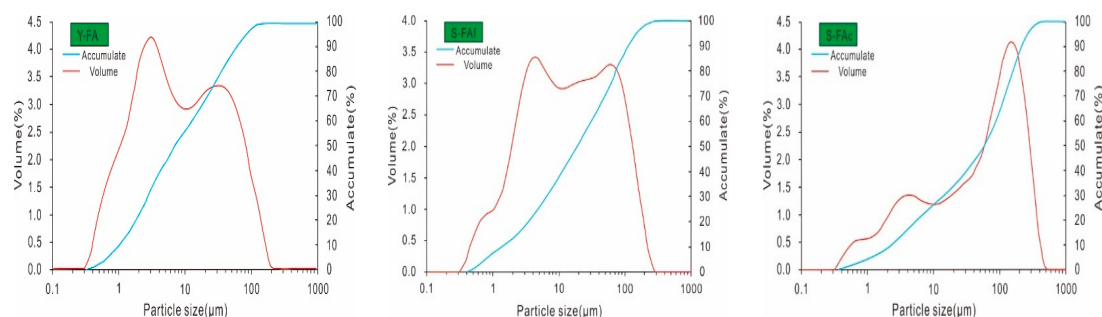


**Figure 4.** Particle-size distribution of Y-FA, S-FAf, and S-FAc. Y-FA, fly ash from Yihua power plant; S-FAf and S-FAc, fine fly ash and coarse fly ash from Shenhua power plant.

The moisture of fly ash and slag samples is very low (0.02–0.9%) and falls within the ranges determines for EU fly ashes (Table 3). Moisture content of the over-drying process after sampling. Y-FA shows the highest moisture (0.9 Faf is similar to FAc, but low to Y-FA. The moisture content of slag is close to 0, probably owing to %) among the combustion residues.

**Table 3.** Physic-chemical parameters, quantitative analyses of the major crystalline species and glass composition for fly ash and slag samples from Shenhua and Yihua power plants.

%	Y-FA	Y-Slag	S-FAf	S-FAc	S-Slag	EU Fly Ashes *
Moisture	0.9	0.02	0.5	0.5	0.1	0–2.4
LOI	5.4	0.1	3.6	3.4	0.6	1.1–8.1
Crystalline species						
Amorphous phase	86.5	75	83.0	77.6	56.0	48–89
Quartz	0.4	8	4.8	6.4	7.2	1.7–13
Mullite	<dl	<dl	6.5	7.5	9.9	3.2–40
Calcite	8.5	<dl	2.2	3.3	3.3	<0.3–0.6
Lime	0.2	<dl	0.6	0.8	<dl	<0.3–5.8
Periclase	1.1	<dl	1.0	1.7	<dl	nd
Anhydrite	2.6	<dl	1.9	2.5	<dl	0.2–15
Magnetite	0.1	<dl	<dl	0.2	<dl	0.1–5.0
Anorthite	<dl	4.6	<dl	<dl	23.6	nd
Hematite	0.6	<dl	<dl	<dl	<dl	2.5–5.9
Augite	<dl	12.4	<dl	<dl	<dl	nd
Glass composition						
SiO <sub>2</sub>	52.5	54.1	45.3	45.6	49.8	31.4–65.5
Al <sub>2</sub> O <sub>3</sub>	12.9	11.0	18.5	18.7	19.6	5.4–29.1
CaO	22.6	10.9	13.2	14.8	8.6	0.6–24.4
Fe <sub>2</sub> O <sub>3</sub>	6.1	9.3	8.6	6.9	10.5	4.1–15.9
SO <sub>3</sub>	3.9	0.3	1.9	1.8	0.7	<0.1–1.6
SiO <sub>2</sub> /Al <sub>2</sub> O <sub>3</sub>	4.1	4.9	2.4	2.4	2.5	1.1–9.4

<dl: under detected limit; nd: no data. \* Data from Moneno et al. [52].

The loss on ignition (LOI) values of fly ash and slag samples fall within the lower range of European fly ashes [52] or even below the minimum value. Y-FA shows the highest LOI value (5.3%) while those of S-FAf, S-FAc, Y-Slag, and S-Slag are 3.6%, 3.4%, 0.1%, and 0.6% respectively. The LOI values of fly ash are greater than that of slag, which is not only related to destruction of the unburned carbon present, but also to breakdown of mineral phases (e.g., decomposition of carbonates, oxidation of sulfides, release of structure water from clay minerals, and dehydration of lime) and to water physically adsorbed on measured samples (e.g., CaO that is rich in fluidized-bed combustion (FBC) ashes) [53].

Both fly ash and slag samples from Shenhua and Yihua power plants demonstrate typical aluminosilicate compositions, with SiO<sub>2</sub> contents higher than those of iron and aluminum oxides. The total content of SiO<sub>2</sub>, Al<sub>2</sub>O<sub>3</sub>, and Fe<sub>2</sub>O<sub>3</sub> is 72.4%, 71.2% and 71.5%, respectively in S-FAf, S-FAc and Y-FA, which is slightly lower than that in the S-Slag (79.9%) and Y-Slag (74.4%). The major element composition indicates that Shenhua and Yihua power plants produces Class F fly ash, characterized by SiO<sub>2</sub> + Al<sub>2</sub>O<sub>3</sub> + Fe<sub>2</sub>O<sub>3</sub> ≥ 70%, and LOI < 6% [54]. It is worth nothing that Class F fly ash is usually considered to be a combustion product of higher rank coals, while Class C fly ash generally comes from the combustion of lower rank coals [55]. The determining factor, however, should be the major element composition rather than the source coal rank.]

### 3.2.2. Mineralogical Characteristics

The characteristics of fly ash are to some extent dependent on the elemental concentrations and modes of element occurrence in feed coals as well as on the combustion conditions [22,56–59]. Fly ash and slag produced from the same feed coal generally have a similar chemical composition, but in common cases, different particle sizes and phase compositions [58]. With respect to fly ash samples, both S-FAf, S-FAc and Y-FA are made up of a predominant Al–Si–Ca–Fe amorphous glass matrix (83%, 77.6% and 86.5% respectively), with different proportions of quartz, mullite (3Al<sub>2</sub>O<sub>3</sub>·2SiO<sub>2</sub>), calcite (CaCO<sub>3</sub>) as major crystalline components (Table 3; Figure 5a,b). Lime (CaO), periclase (MgO), anhydrite (CaSO<sub>4</sub>) are present in much lower proportions, and magnetite was also detected in S-FAc and Y-FA. Although not detected by XRD, BaSO<sub>4</sub> and SrSO<sub>4</sub> were observed under SEM-EDX in three fly ashes (Figure 5f,j,g,h,n,o,p). The occurrence of BaSO<sub>4</sub> and SrSO<sub>4</sub> is probably attributed to the high content of Sr and Ba in the feed coals, which is mainly fed with Junngar coal. Moreover, plerosphere, cenosphere and unburned carbon can also be observed by SEM-EDX in fly ashes (Figure 5k,m). Cenospheres are one of the most desired byproducts of coal combustion process nowadays [60]. It has a hollow spherical structure and can be applied in a wide range of industrial applications, due to their superior properties; such as low bulk density, high thermal resistance, high workability and high strength [61]. Plerosphere is a typical fly ash structure, which can be formed due to capture of microspheres by a cenosphere during combustion [62]. Plerosphere with a quantity of hollow microspheres both can reduce the emission of fine particles into the atmosphere and enrich elements inside itself.

As aforementioned, the glass matrix content of S-FAf and Y-FA is high, however, the content of crystalline components is lower than that of S-FAc, which may be attributed to the larger grain size and pores of the coarse ash when compared to those of fine ash, forasmuch minerals tend to crystallize in the pores of coarse ash.

When compared with EU fly ashes [48], the content of crystal minerals in fly ash basically falls in the low EU range, nevertheless glass matrix contents are in the upper range of EU fly ashes. Fly ash has high calcite content, which may be attributed to the high calcite content in feed coal, or because of the calcite formed by adding lime in the flue gas desulfurization device. The occurrence of mullite is attributed to the decomposition of kaolinite, illite, and other clay minerals in the coals. The higher content of mullite in fly ash corresponds to the higher characteristics of aluminum minerals in feed coals. The occurrence of lime is due to the decomposition of feed-coal calcite into CaO and CO<sub>2</sub> at around 900 °C. The occurrence of periclase is usually related to the presence of MgO in fly ash.

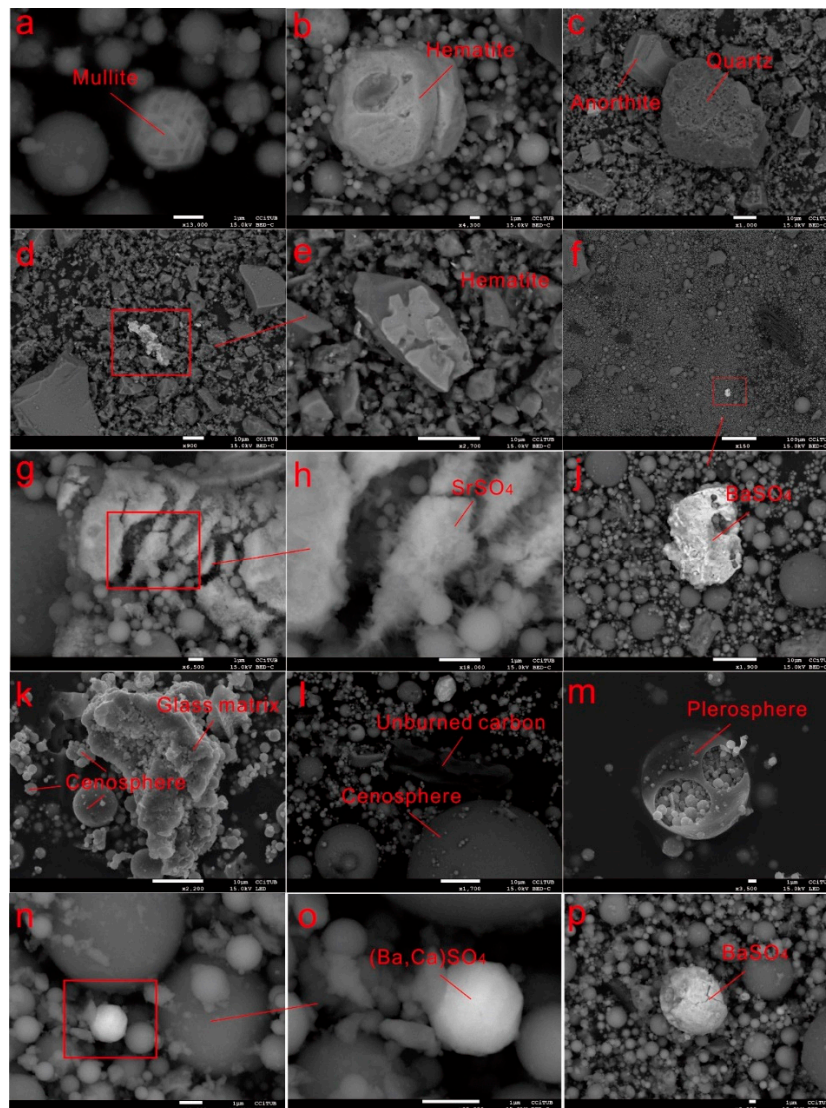


**Figure 5.** Scanning electron microscope (SEM) image of minerals in fly ash and slag. **a:** Mullite in S-FAf; **b:** Hematite in S-FAC; **c:** Anorthite and quartz in slag; **d,e:** Hematite in slag; **f,j:** BaSO<sub>4</sub> in S-FAC; **g, h:** SrSO<sub>4</sub> in S-FAf; **k:** Glass matrix and cenosphere in S-FAf; **l:** Unburned carbon and cenosphere in S-FAf; **m:** Plerosphere in S-FAf; **n,o:** (Ba, Ca)SO<sub>4</sub> in Y-FA; and **p:** BaSO<sub>4</sub> in Y-FA.

With respect to slag sample, S-Slag and Y-Slag also contains aluminium–silicate amorphous glass matrix as major constituent (56%, 75% respectively). S-Slag has variable contents of anorthite and mullite as the main crystalline phases (Table 4). Furthermore, quartz and calcite are also present in minor proportions. The content of mullite, quartz and calcite in slag is higher than those of fly ash, while quartz and hematite can be detected in microscopic perspective under SEM (Figure 5c–e). Y-Slag is made up of quartz, anorthite and augite as crystalline phases (Table 4). Significantly, the anorthite content in the S-Slag and Y-Slag reaches 23.6% and 4.6%. Although the content of sodium and calcium in fly ash is higher than that in slag, anorthite content is much higher in slag than in fly ash, indicating that the majority of anorthite is formed from a combination of aluminosilicate matrix and sodium calcium oxide in slag. Similarly, augite is formed from the cooling crystallization of aluminosilicate.

**Table 4.** Major and trace element concentrations of fly ash and slag samples for Shenhua and Yihua power plants.

%	Y-FA	Y-Slag	S-FAf	S-FAc	S-Slag	EU Fly Ashes *
Al	6.8	5.8	9.8	9.9	10.4	9.3–18.8
Ca	16.1	7.8	9.4	10.6	6.1	0.4–19.5
Fe	4.3	6.5	6.1	4.8	7.3	1.8–11.2
K	0.9	1.1	0.5	0.5	0.5	0.3–3.3
Mg	2.2	0.9	1.7	2.1	0.9	0.4–2.3
Na	2.9	2.5	1.5	1.9	1	0.1–0.9
S	1.6	0.1	0.7	0.7	0.3	0.0–3.4
P	0.1	0.1	0.2	0.2	0.2	nd
Ti	0.4	0.3	0.6	0.5	0.6	nd
Mn	0.1	<dl	0.1	0.1	0.1	nd
mg/kg						
Li	29.8	22.8	33	40.8	32.1	36–377
Be	2.4	1.8	2.2	2.7	2.2	3–34
B	635.3	39.0	452	710	100	24–534
Sc	7.5	6.1	16.5	15.6	15.6	nd
V	77.4	59.9	155	154	122	14–514
Cr	58.4	35.8	81.8	89.8	74.8	47–281
Co	42.0	30.1	27.7	26	22.8	20–112
Ni	81.6	53.9	60.1	60.2	54	49–377
Cu	46.7	29.4	99.4	99.4	<dl	39–254
Zn	163.4	53.2	113	109	66.8	70–924
Ga	13.8	5.9	21.6	24.5	10.1	nd
Ge	4.2	1.1	3.1	2.8	<dl	1–61
As	18.1	10.0	17.6	21.7	7.4	22–162
Se	36.7	<dl	2.9	2	<dl	3–30
Rb	31.6	35.5	24.4	25.5	25.4	22–202
Sr	3351.8	2289.5	2889	3299	2127	131–4406
Y	23.4	24.2	33.6	34.3	33.3	nd
Zr	93.0	158.5	182	180	182	nd
Nb	3.6	6.1	9.2	6.2	10.6	nd
Mo	2.3	1.2	4.5	5	1.9	5–22
Cd	<dl	<dl	<dl	<dl	<dl	1–6
Sn	2.2	0.9	3.2	3.3	1	4–15
Sb	2.5	<dl	1.5	1.4	<dl	1–120
Cs	2.2	1.4	3.6	3.8	3.8	nd
Ba	3435.2	2302.7	2743	2182	2568	311–3134
La	25.1	28.7	44.8	46.4	45.6	nd
Ce	47.7	56.2	82.3	86.8	84.6	nd
Pr	5.3	6.5	9.6	10	9.7	nd
Nd	20.8	26.0	37.1	39.4	37.8	nd
Sm	4.8	6.0	8.2	8.7	8.1	nd
Eu	1.3	1.5	1.9	1.9	2	nd
Gd	4.4	5.3	7.4	7.6	7.4	nd
Tb	<dl	<dl	1	1	1	nd
Dy	4.1	4.6	6.2	6.3	6.1	nd
Ho	0.8	0.9	1.2	1.2	1.2	nd
Er	2.3	2.4	3.3	3.4	3.3	nd
Tm	<dl	<dl	0.9	0.9	0.9	nd
Yb	2.5	2.5	3.4	3.4	3.3	nd
Lu	<dl	<dl	<dl	<dl	<dl	nd
Hf	3.0	4.1	4.9	5	5	nd
Ta	<dl	<dl	<dl	<dl	<dl	nd
W	4.7	1.0	3.4	5	1.7	nd
Tl	0.9	<dl	<dl	0.8	<dl	nd
Pb	21.8	3.9	26.5	31.4	4.7	40–1075
Bi	<dl	<dl	<dl	<dl	<dl	nd
Th	5.7	5.6	11.4	11.3	11.1	17–65
U	2.3	1.8	4	4.4	3.2	5–29

&lt;dl: under detected limit; nd: no data.

### 3.2.3. Geochemical Characteristics

As demonstrated in Table 4, the concentrations of Ca and S are higher in fly ash than in slag, which is consistent with the previous study that fly ash samples have higher content of anhydrite than slag. The concentration of Fe shows an opposite trend, due to the density of iron, or to the formation of magnetite at high temperatures. With the exception of Ca, S and Fe, the concentrations of other elements in fly ash samples are approximate to that in slag samples. When compared with the concentrations of major oxides in EU fly ashes [48], Na concentrations in three fly ashes and two slags are higher than its maximum value in EU fly ashes. Aluminum, Ca, Fe, K, Mg and S concentrations fall within the middle concentration range of EU fly ashes.

Overall, the concentrations of trace elements in CCPs are very low. When compared with the average values of EU fly ashes, concentrations of most trace elements in fly ashes and slags are between the corresponding 25th percentile (P25) and P75 values of EU fly ashes (Figure 6), and those of some elements, such as Li, Be, V, Cr, Co, Ni, Zn, As, Se, Rb, Mo, Cd, Sn, Sb, Th and U are even lower than or similar to the corresponding P25 values of EU fly ashes (Figure 6). Furthermore, the contents of Be, As, Se, Cd, Sn, Th, U in fly ash are even lower than or close to the minimum values of EU fly ash. Nonetheless, B, Sr and Ba in three fly ashes show higher concentrations, greater than or similar to the maximum values of EU fly ashes. As regards Yihua power plant, the concentrations of most elements are higher in Y-FA than in Y-Slag with the exception of Fe, K, Y, Zr and Nb (Table 4). Comparing the element concentrations between S-FAf and S-FAc from Shenhua power plant, with the exception of Li, B, Cr, Sr and Pb, the concentrations of most elements are higher in S-FAf than in S-FAc, which is consistent with previous studies [37,45,47]. It is worth noting that because of the REY non-volatile properties during coal combustion, the REY are not expected to partition between fly ash, bottom ash, and slag [18].

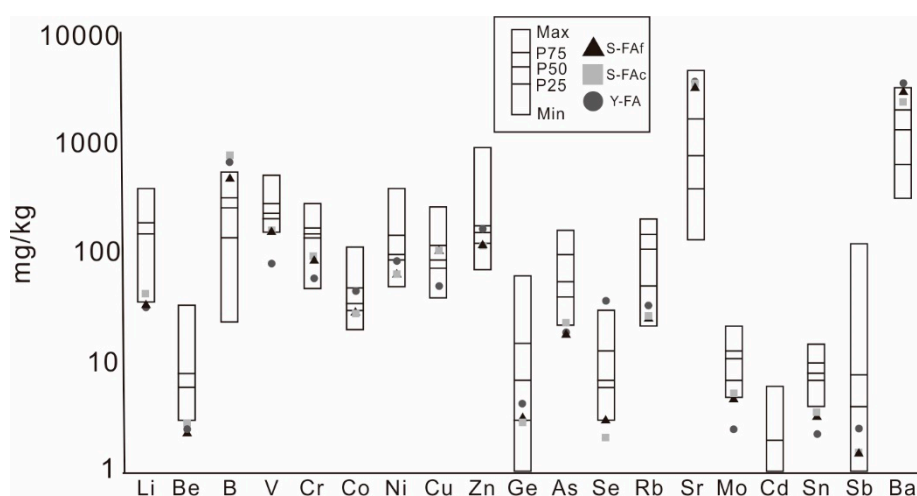


**Figure 6.** Concentrations of selected trace elements in the fly ashes at Shenhua and Yihua power plants compared with the corresponding maximum, minimum, P25, P50, and P75 values in European fly ashes [52].

### 3.3. Enrichment and Partitioning of Major and Trace Elements

According to the EF calculated on the strength of element concentrations in feed coals, elements can be classified as four groups in both power plants (Table 5, Figure 7).

**Table 5.** Enrichment factors (EF) and total enrichment factors (EF<sub>T</sub>) of major and trace elements for Shenhua power plants and Yihua power plants. EF<sub>AS</sub>, EF<sub>AY</sub> enrichment factor in fly ash from Shenhua power plant and Yihua power plant respectively; EF<sub>SS</sub>, EF<sub>SY</sub> enrichment factor in slag from Shenhua power plant and Yihua power plant respectively; EF<sub>TS</sub>, EF<sub>TY</sub> total enrichment factors of major and trace elements for Shenhua power plants and Yihua power plant respectively.

	EF <sub>AY</sub>	EF <sub>SY</sub>	EF <sub>TY</sub>	EF <sub>AS</sub>	EF <sub>SS</sub>	EF <sub>TS</sub>		EF <sub>AY</sub>	EF <sub>SY</sub>	EF <sub>TY</sub>	EF <sub>AS</sub>	EF <sub>SS</sub>	EF <sub>TS</sub>
Al	1.0	1.0	1.0	1.0	1.0	1.0	Ga	nd	nd	nd	1.4	0.6	1.3
Ca	1.2	0.7	1.1	1.3	0.8	1.3	As	1.1	0.7	1.1	0.8	0.3	0.7
Fe	2.2	4.0	2.4	1.2	1.6	1.3	Rb	1.0	1.3	1.0	0.9	0.8	0.9
K	0.9	1.3	0.9	0.8	0.8	0.8	Sr	1.4	1.1	1.4	1.5	1	1.5
Mg	0.9	0.4	0.9	1.5	0.6	1.4	Y	1.1	1.3	1.1	1.1	1.1	1.1
Na	0.8	0.8	0.8	1.6	0.9	1.5	Zr	1.1	1.3	0.8	0.8	0.8	0.8
S	0.5	0.0	0.5	0.2	0.1	0.2	Nb	nd	nd	nd	0.7	1	0.7
P	1.3	1.0	1.3	1.1	0.7	1.0	Ba	6.9	5.4	6.7	1.1	1.1	1.1
Ti	1.0	0.9	1.0	1.2	1.1	1.2	La	1.0	1.1	1.0	1.1	1.0	1.1
Mn	1.4	1.3	1.4	1.4	1.4	1.4	Ce	1.0	1.4	1.1	1.1	1.1	1.1
Li	1.0	0.9	1.0	1.3	1	1.3	Pr	nd	nd	nd	1.1	1	1.1
B	0.8	0.1	0.8	2.0	0.3	1.8	Nd	1.0	1.5	1.1	1.1	1.1	1.1
V	1.1	1.0	1.1	1.1	0.8	1	Sm	nd	nd	nd	1.1	1	1.1
Cr	1.2	0.8	1.1	1.3	1.1	1.3	Gd	nd	nd	nd	1.2	1.1	1.1
Co	0.8	0.6	0.7	1.2	0.9	1.1	Dy	1.2	1.2		1.2	1.1	1.2
Ni	1.1	0.9	1.1	1.4	1.2	1.4	Pb	1.9	0.4	1.7	1.2	0.2	1.1
Cu	1.6	1.2	1.6	0.9	0	0.8	Th	nd	nd	nd	1	0.9	1
Zn	0.8	0.3	0.7	1	0.6	1							

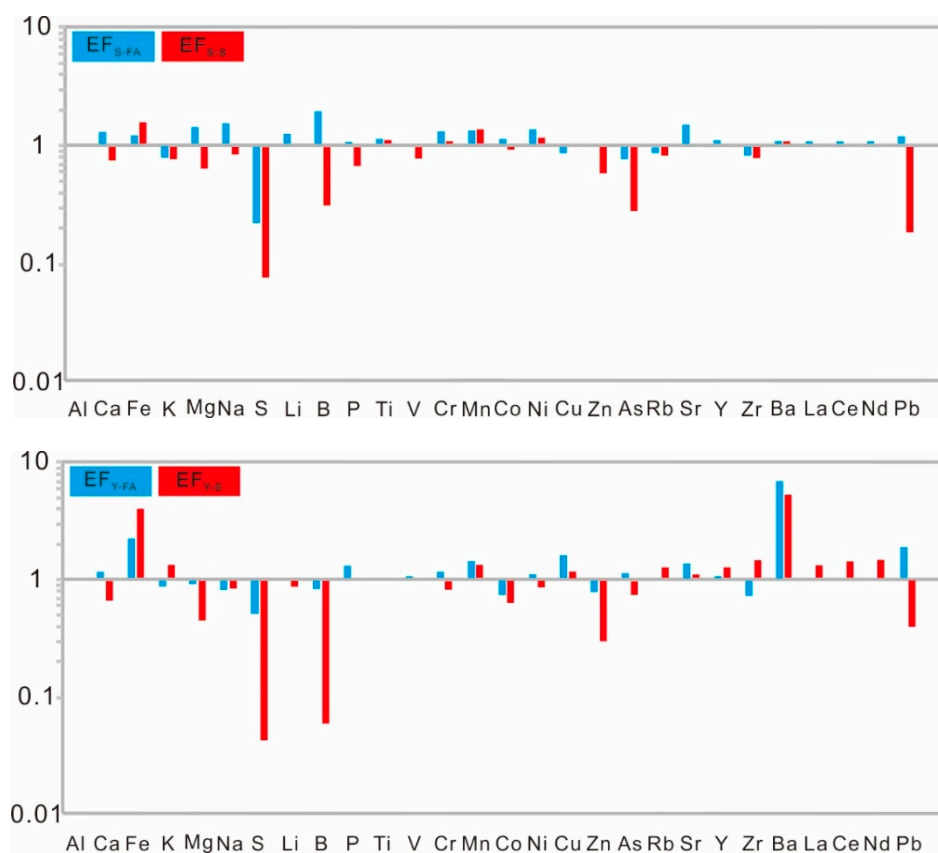


**Figure 7.** Enrichment factors for fly ash and slag from Shenhua (up) and Yihua (down) power plants. EF<sub>S-FA</sub>, enrichment factor in fly ash from Shenhua power plant; EF<sub>S-S</sub>, enrichment factor in slag from Shenhua power plant; EF<sub>Y-FA</sub>, enrichment factor in fly ash from Yihua power plant; EF<sub>Y-S</sub>, enrichment factor in slag from Yihua power plant.

For the Shenhua power plant, the elements are classified as follows:

(a) Elements abounded in fly ash and exhausted in slag: Ca, Mg, Na, B, P, Co, Ga, Pb; (b) elements abounded in slag and exhausted in fly ash: Fe; (c) elements with unapparent abundance or exhaustion in fly ash and slag: Ti, V, Zn, Th, Ba and REEs; (d) elements exhausted in both fly ash and slag: K, S, Cu, As, Rb, Zr, Nb.

Likewise, for the Yihua power plant, the elements are classified as follows:

(a) Elements abounded in fly ash and exhausted in slag: Ca, Cr, Ni, As, Pb; (b) elements abounded in slag and exhausted in fly ash: Fe, K, Zr; (c) elements with unapparent abundance or exhaustion in fly ash and slag: P, Ti, Li, V, Ni, Ba and REEs; (d) elements exhausted in both fly ash and slag: Mg, Na, B, Co, Zn, S. The elements which are abounded in fly ash and exhausted in slag, displaying volatile or semi-volatile behavior during the combustion process, then condensing in the fly ash through ESP (the temperature falls from 1300 °C to about 150 °C). Ca and Pb are the commonable elements in this group at both power plants. Mg, Na, B, P, Co and Ga are enriched in fly ash at the Shenhua power plant and Cr, Ni, and As at the Yihua power plant. As described above, the reason why Fe is enriched in slag and exhausted in fly ash at both power plants is because of its high density and/or reactivity to be magnetic. The elements without abundance in fly ash or slag are those that typically exhibit non-volatile behavior during combustion. It is those volatile elements in coal combustion that are partly exhausted in both fly ash and slag, especially S. As mentioned above, As, Nb, Zr, Cu and K present exhaustion at the Shenhua power plant, suggesting that the ESP temperature is too high for As and other elements to condense out of the gas stream. At Yihua power plant, Mg is exhausted both in fly ash and slag, together with Na, B, Co and Zn. The partial volatility of these elements may be attributed to a higher ESP temperature at the Yihua than at the Shenhua power plant.

The partitioning for major and trace elements at the ESP and boiler in Shenhua and Yihua PCC plants were calculated by normalized Eft with the fly ash (90%) and slag (10%) production (Figure 8). For the Shenhua power plant, S is the element with the highest volatile portion at ESP (80%). However, considering that the retention efficiency of S in general power plants is 90%, the content of S discharged into the atmosphere is about 8%, 72% of which is retained in the FGD device, with most of the remaining S reserved in the fly ash. As (30%), Nb (30%), Zr (20%), Cu (20%), and K (20%) also to some extent exhibit partial volatile proportions. The volatility of As, Nb, Zr, Cu and K may be due to the presence of highly volatile metal chlorides, and the temperature of ESP is high.

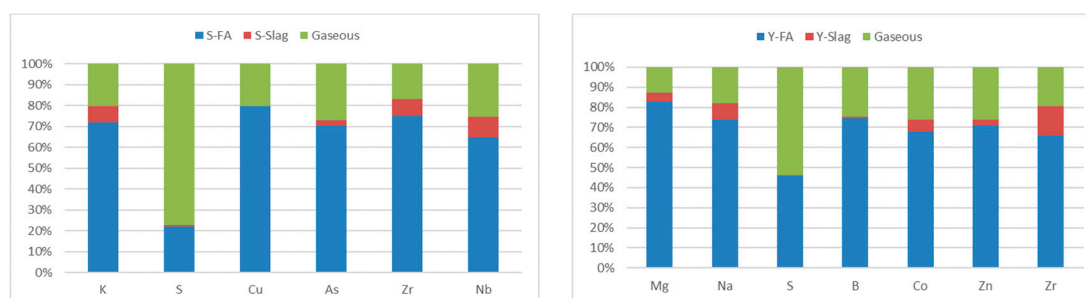


**Figure 8.** Partitioning for some volatile elements at ESP at Shenhua (left) and Yihua (right) power plants.

As regards the Yihua plant, S shows similar partitioning as at the Shenhua plant, with the highest volatile fraction (54%), and as described for the Shenhua plant, only 5% of S is emitted into the atmosphere, whereas 49% of S is retained in the FGD. The remaining S is all retained in fly ash. The higher volatile fraction of S at the Shenhua plant may be due to a lower content of Ca. Mg (13%), Na (18%), B (25%), Co (26%), and Zr (20%) also display relatively high volatile proportions. The remaining elements of two power plants have no obvious volatile behavior, furthermore, when compared with the concentrations of elements in slag, and more than 70% partition of each element is retained in fly ash because of the much higher production of fly ash in regard to slag.

### 3.4. Leaching Potential

The leaching experiment simulates the process of different elements' dissolution and migration of CCPs, which are piled in open space and leached by natural rain (acid rain). Subsequently, the concentrations of elements in leaching solution were determined by ICP-AES and ICP-MS to reveal the occurrence mode and migration characteristics of various elements in CCPs (Table 6). Most elements are capable of leaching, and according to the European Council Decision 2003/33/EC [46], whether the element content is hazardous or not is classified after leaching experiment. The leachable concentrations of Ca, Mg, Na, S and Si (major elements) as well as B, Cr, Mn, Se, Sr, Mo, Ba (trace elements) in CCPs from both power plants are comparatively high, falling within inert to non-hazardous range for landfill materials. The concentrations of Cr, Se, Mo, and Ba from S-FAf are considered as non-hazardous landfill materials, and those of remaining elements fall within the inert range for landfill materials. In terms of leachability of elements, the leachable concentrations of most trace elements are higher in S-FAf than in S-FAc, and slag presents the lowest leachability, which is relevant to the concentrations of elements present in corresponding samples. Overall, CCPs from the Shenhua and Yihua power plant belong to inert landfill materials, indicating that they can be utilized with low environmental implication.

**Table 6.** Element concentrations of fly ash and slag leachates compared with EU fly ash leachates [52] and inert, non-hazardous, and hazardous limit values of some toxic elements for landfill materials.

ppm						Limit values 2003/33/CE [43]		
	Y-FA	Y-Slag	S-FAf	S-FAc	S-Slag	Inert	Non-Hazardous	Hazardous
Al	5.8	3.9	<dl	<dl	0.2			
Ca	32.4	382.0	4688	3702	1611			
Fe	<dl	<dl	<dl	<dl	<dl			
K	331.6	7.6	7.4	5.1	16.2			
Mg	0.6	3.3	0.1	0.1	113			
Mn	<dl	<dl	<dl	<dl	<dl			
Na	3428.8	142.2	333	191	146			
P	<dl	<dl	<dl	<dl	<dl			
S	1020.0	201.8	578	21.2	1508			
Si	114.5	112.6	0.8	0.6	31.1			
<b>ppb</b>								
Li	75.1	<dl	250	228	257			
Be	<dl	<dl	<dl	<dl	<dl			
B	8186.6	16.0	2354	694	17,448			
Sc	<dl	<dl	<dl	<dl	<dl			
Ti	<dl	<dl	<dl	<dl	<dl			
V	215.9	<dl	23.8	30.8	88.4			
Cr	59.8	<dl	1605	206	<dl	500	10,000	70,000
Mn	<dl	<dl	<dl	<dl	34.3			
Co	<dl	<dl	<dl	<dl	<dl			
Ni	<dl	<dl	24.6	11.4	12.2	400	10,000	40,000
Cu	4.1	0.1	<dl	8.3	44.8	2000	50,000	100,000
Zn	<dl	18.8	<dl	<dl	57.7	4000	50,000	200,000
Ga	<dl	<dl	<dl	234	4.0			
Ge	<dl	<dl	<dl	<dl	<dl			
As	68.1	<dl	<dl	5.7	22.0	500	2000	25,000
Se	0.0	<dl	164	5.8	<dl	100	500	7000
Rb	11.6	<dl	23.4	24.9	27.5			
Sr	8382.5	2.0	292,448	487,672	81,989			
Y	<dl	<dl	<dl	<dl	<dl			
Zr	<dl	<dl	<dl	<dl	<dl			
Nb	<dl	<dl	<dl	<dl	<dl			
Mo	10.6	<dl	897	223	27.4	500	10,000	30,000

Table 6. Cont.

ppm	Y-FA	Y-Slag	S-FAf	S-FAc	S-Slag	Inert	Limit values 2003/33/CE [43]	
							Non-Hazardous	Hazardous
Cd	<dl	<dl	<dl	<dl	<dl	40	1000	5000
Sn	<dl	<dl	<dl	<dl	<dl			
Sb	<dl	<dl	<dl	<dl	19.1	60	700	5000
Cs	<dl	<dl	<dl	<dl	<dl			
Ba	485.8	<dl	3552	104,720	749	2000	100,000	300,000
Hf	<dl	<dl	<dl	<dl	<dl			
W	24.2	<dl	<dl	<dl	<dl			
Tl	<dl	<dl	<dl	<dl	<dl			
Pb	<dl	<dl	<dl	<dl	<dl	500	10,000	50,000
Th	<dl	<dl	<dl	<dl	<dl			
U	<dl	<dl	<dl	<dl	<dl			

<dl: under detected limit.

At present, many researchers investigate the extraction of various beneficial elements and/or minerals from fly ash [63–66]. The concentrations of B, Sr and Ba in the leaching solution are considerable. It may be a research focus to extract trace scarce elements from the leaching solution of CCPs.

#### 4. Conclusions

The feed coals from two power plants primarily come from Junggar coals, which are characterized by high quality, with low concentrations of potential hazardous elements, so the fly ash and slag generated from combustion of Junggar coals are supposed to pose a little threat to environment.

The fly ash and slag samples are characterized by high glass matrix content, with low concentrations of quartz, mullite, calcite and anhydrite. Traces of Barite and SrSO<sub>4</sub> also occur in fly ashes. Cenospheres and unburned carbon exist in fly ashes, while typical plerosphere was observed only in S-FAf. In terms of major elements, the Na contents from fly ash and slag are higher than the average values of EU fly ashes, whereas the remaining major oxides contents are within those of EU fly ashes. In addition, the concentrations of trace elements in fly ash and slag samples are even lower than their P25 values in EU fly ashes due to lower element content of feed coals.

During coal combustion process, most elements are retained in fly ash in high proportions (>70%) rather than in slag on account of the high fly ash/slag production proportion (90:10). Sulphur is highly volatile at both plants (80%, 54% respectively for Shenhua and Yihua plant), however, most of S is retained in the FGD.

The low concentrations of elements in CCPs lead to low leachable potential, and leachable concentrations of most potential toxic elements are within the range for inert to non-hazardous landfill materials according to the limits regulated by the 2003/33/EC Decision. The CCPs from both power plants are supposed to be utilized with very low environmental burden.

**Author Contributions:** Writing—original draft preparation, P.W.; supervision, X.Z.; formal analysis, B.L., S.Z. and Y.S.; investigation, D.G. and X.M.; methodology, X.Q., N.M. and P.C.; writing—review and English editing, J.L.

**Funding:** This research was funded by National Key R&D Program of China (No. 2018YFF0215400), the National Science Foundation of China (No. 41972179), and the Fundamental Research Funds for the Central Universities, China University of Geosciences (Wuhan) (No. CUGCJ1823).

**Conflicts of Interest:** The authors declare no conflict of interest.

#### References

1. Dai, S.F.; Yan, X.Y.; Ward, C.R.; Hower, J.C.; Zhao, L.; Wang, X.B.; Zhao, L.X.; Ren, D.Y.; Finkelman, R.B. Valuable elements in Chinese coals: A review. *Int. Geol. Rev.* **2018**, *60*, 590–620. [[CrossRef](#)]

2. BP-Statistical Review of World Energy 2019; British Petroleum Company: London, UK, 2019.
3. National Development and Reform Commission (NDRC) and National Energy Administration (NEA). *13th Five-Year Plan of Energy Development*; National Development and Reform Commission (NDRC) and National Energy Administration (NEA): Beijing, China, 2016.
4. Wang, X.S.; Tang, Y.G.; Huan, B.B.; Xu, J.J. Enrichment characteristics of trace elements in coal gasification process in ningdong gasification plant. *Coal Geol. China* **2016**, *28*, 14–18.
5. Department of Energy (DOE), National Energy Technology Laboratory (NETL). *Gasification Technology Database*; Department of Energy (DOE), National Energy Technology Laboratory (NETL): Washington, DC, USA, 2010.
6. Liu, S.Q.; Qi, C.; Jiang, Z.; Zhang, Y.J.; Niu, M.F.; Li, Y.Y.; Dai, S.F.; Finkelman, R.B. Mineralogy and geochemistry of ash and slag from coal gasification in China: A review. *Int. Geol. Rev.* **2018**, *60*, 717–735. [[CrossRef](#)]
7. EhsanMunawer, M. Human health and environmental impacts of coal combustion and post-combustion wastes. *J. Sustain. Min.* **2018**, *17*, 87–96.
8. Finkelman, R.B.; Tian, L.W. The health impacts of coal use in China. *Int. Geol. Rev.* **2018**, *60*, 579–589. [[CrossRef](#)]
9. Li, J.; Zhuang, X.G.; Querol, X.; Font, O.; Moreno, N. A review on the applications of coal combustion products in China. *Int. Geol. Rev.* **2018**, *60*, 671–716. [[CrossRef](#)]
10. Ahmaruzzaman, M. A review on the utilization of fly ash. *Prog. Energy Combust. Sci.* **2010**, *36*, 327–363. [[CrossRef](#)]
11. Zhao, Y.C.; Ma, S.M.; Yang, J.P.; Zhang, J.Y.; Zheng, C.G. The development and status quo of super net emission of pollutants from coal-fired power plants. *J. Coal* **2015**, *40*, 2629–2640.
12. Cox, M.; Nugteren, H.; Janssen-Jurkovičová, M. *Combustion Residues-Current, Novel and Renewable Applications*; John Wiley & Sons Ltd.: Chichester, UK, 2008.
13. Heidrich, C.; Feuerborn, H.; Weir, A. *Coal Combustion Products—A Global Perspective*; VGB Power Tech.: Essen, Germany, 2013.
14. Koukouzas, N.K.; Zeng, R.S.; Perdikatsis, V.; Xu, W.D.; Kakaras, E.K. Mineralogy and geochemistry of Greek and Chinese coal fly ash. *Fuel* **2006**, *85*, 2301–2309. [[CrossRef](#)]
15. Li, H.L.; Zhang, W.L.; Wang, J.; Yang, Z.Q.; Li, L.Q.; Shih, K.M. Copper slag as a catalyst for mercury oxidation in coal combustion flue gas. *Waste Manag.* **2018**, *74*, 253–259. [[CrossRef](#)] [[PubMed](#)]
16. Pandey, V.C.; Singh, N. Impact of fly ash incorporation in soil systems. *Agric. Ecosyst. Environ.* **2010**, *136*, 16–27. [[CrossRef](#)]
17. Belviso, C.; Cavalcante, F.; Di Gennaro, S.; Palma, A.; Ragone, P.; Fiore, S. Mobility of trace elements in fly ash and in zeolitised coal fly ash. *Fuel* **2015**, *144*, 369–379. [[CrossRef](#)]
18. Dai, S.F.; Finkelman, R.B. Coal as a promising source of critical elements: Progress and future prospects. *Int. J. Coal Geol.* **2018**, *186*, 155–164. [[CrossRef](#)]
19. Stuckman, M.Y.; Lopano, C.L.; Granite, E.J. Distribution and speciation of rare earth elements in coal combustion by-products via synchrotron microscopy and spectroscopy. *Int. J. Coal Geol.* **2018**, *195*, 125–138. [[CrossRef](#)]
20. Kolker, A.; Scott, C.; Hower, J.C.; Vazquez, J.A.; Lopano, C.L.; Dai, S.F. Distribution of rare earth elements in coal combustion fly ash, determined by SHRIMP-RG ion microprobe. *Int. J. Coal Geol.* **2017**, *184*, 1–10. [[CrossRef](#)]
21. Seredin, V.V.; Dai, S.F. The occurrence of gold in fly ash derived from high-Ge coal. *Miner. Depos.* **2014**, *49*, 1–6. [[CrossRef](#)]
22. Dai, S.F.; Seredin, V.V.; Ward, C.R.; Jiang, J.H.; Hower, J.C.; Song, X.L.; Jiang, Y.F.; Wang, X.B.; Gornostaeva, T.; Li, X.; et al. Composition and modes of occurrence of minerals and elements in coal combustion products derived from high-Ge coals. *Int. J. Coal Geol.* **2014**, *121*, 79–97. [[CrossRef](#)]
23. Laudal, D.A.; Benson, S.A.; Addleman, R.S.; Palo, D. Leaching behavior of rare earth elements in fort union lignite coals of North America. *Int. J. Coal Geol.* **2018**, *191*, 112–124. [[CrossRef](#)]
24. Zhang, W.C.; Honaker, R.Q. Rare earth elements recovery using staged precipitation from a leachate generated from coarse coal refuse. *Int. J. Coal Geol.* **2018**, *195*, 189–199. [[CrossRef](#)]

25. Zhou, J.B.; Zhuang, X.G.; Alastuey, A.; Querol, X.; Li, J.H. Geochemistry and mineralogy of coal in the recently explored Zhundong large coal field in the Junggar basin, Xinjiang province, China. *Int. J. Coal Geol.* **2010**, *82*, 51–67. [[CrossRef](#)]
26. Li, J.; Zhuang, X.G.; Querol, X.; Font, O.; Moreno, N.; Zhou, J.B.; Lei, G.M. High quality of Jurassic Coals in the Southern and Eastern Junggar Coalfields, Xinjiang, NW China: Geochemical and mineralogical characteristics. *Int. J. Coal Geol.* **2012**, *99*, 1–15. [[CrossRef](#)]
27. Song, H.; Ni, S.J.; Chi, G.X.; Zhang, C.J.; Hou, M.C.; Liu, H.X.; Wang, G.; Yan, W.Q. Systematic variations of H-O-C isotopes in different alteration zones of sandstone-hosted uranium deposits in the southern margin of the Yili Basin (Xinjiang, China): A review and implications for the ore-forming mechanisms. *Ore Geol. Rev.* **2019**, *107*, 615–628. [[CrossRef](#)]
28. Chen, H.Y.; Wan, B.; Pirajno, F.; Chen, Y.J.; Xiao, B. Metallogensis of the Xinjiang Orogens, NW China—New discoveries and ore genesis. *Ore Geol. Rev.* **2018**, *100*, 1–11. [[CrossRef](#)]
29. Dai, S.F.; Yang, J.Y.; Ward, C.R.; Hower, J.C.; Liu, H.D.; Garrison, T.M.; French, D.; O’Keefe, J.M.K. Geochemical and mineralogical evidence for a coal-hosted uranium deposit in the Yili Basin, Xinjiang, northwestern China. *Ore Geol. Rev.* **2015**, *70*, 1–30. [[CrossRef](#)]
30. Qi, X.B.; Song, G.L.; Yang, S.B.; Yang, Z.; Lyu, Q.G. Migration and transformation of sodium and chlorine in high-sodium high-chlorine Xinjiang lignite during circulating fluidized bed combustion. *J. Energy Inst.* **2019**, *92*, 673–681. [[CrossRef](#)]
31. Zhang, Y.Y.; Tian, J.J.; Feng, S.; Yang, F.; Lu, X.Y. The occurrence modes and geologic origins of arsenic in coal from Santanghu Coalfield, Xinjiang. *J. Geochem. Explor.* **2018**, *186*, 225–234. [[CrossRef](#)]
32. Zhao, H.Y.; Wang, B.Z.; Li, Y.H.; Song, Q.; Zhao, Y.Q.; Zhang, R.Y.; Hu, Y.; Liu, S.C.; Wang, X.H.; Shu, X.Q. Effect of chemical fractionation treatment on structure and characteristics of pyrolysis products of Xinjiang long flame coal. *Fuel* **2018**, *234*, 1193–1204. [[CrossRef](#)]
33. Dai, B.Q.; Wu, X.J.; Zhao, J.; Zhang, L. Xinjiang lignite ash slagging and flow under the weak reducing environment at high temperatures—Slag viscosity and its variation with ash type and addition of clay. *Fuel* **2019**, *245*, 438–446. [[CrossRef](#)]
34. Izquierdo, M.; Querol, X. Leaching behaviour of elements from coal combustion fly ash: An overview. *Int. J. Coal Geol.* **2012**, *94*, 54–66. [[CrossRef](#)]
35. Zhang, S.; Dai, S.; Finkelman, R.B.; Graham, I.T.; French, D.; Hower, J.C.; Li, X. Leaching characteristics of alkaline coal combustion by-products: A case study from a coal-fired power plant, Hebei Province, China. *Fuel* **2019**, *255*, 115710. [[CrossRef](#)]
36. Yang, Z.; Wang, C.; Liu, D.; Li, Y.; Ning, Y.; Yang, S.; Zhang, Y.; Tang, Y.; Tang, Z.; Zhang, W. Investigation of elements (U, V, Sr, Ga, Cs and Rb) leaching and mobility in uranium-enriched coal ash with thermochemical treatment. *J. Clean. Prod.* **2019**, *233*, 115–125. [[CrossRef](#)]
37. Li, J.; Zhuang, X.G.; Querol, X.; Font, O.; Moreno, N.; Zhou, J.B. Environmental geochemistry of the feed coals and their combustion by-products from two coal-fired power plants in Xinjiang Province, Northwest China. *Fuel* **2012**, *95*, 446–456. [[CrossRef](#)]
38. Tang, M.C.; Zhou, C.C.; Pan, J.H.; Zhang, N.N.; Liu, C.; Cao, S.S.; Hu, T.T.; Ji, W.S. Study on extraction of rare earth elements from coal fly ash through alkali fusion—Acid leaching. *Miner. Eng.* **2019**, *136*, 36–42. [[CrossRef](#)]
39. *Standard Test Method for Moisture in the Analysis Sample of Coal and Coke*; ASTM International: West Conshohocken, PA, USA, 2011; No. ASTM D3173-11.
40. *Standard Test Method for Ash in the Analysis Sample of Coal and Coke from Coal*; ASTM International: West Conshohocken, PA, USA, 2018; No. ASTM D3174-12.
41. *Standard Test Method for Volatile Matter in the Analysis Sample of Coal and Coke*; ASTM International: West Conshohocken, PA, USA, 2018; No. ASTM D3175-18.
42. Chung, F.H. Quantitative interpretation of X-ray diffraction patterns of mixtures: I. Matrix flushing method for quantitative multicomponent analysis. *J. Appl. Crystallogr.* **1974**, *7*, 519–525. [[CrossRef](#)]
43. Querol, X.; Alastuey, A.; Chinchon, J.S.; Turiel, J.L.F.; Soler, A.L. Determination of Pyritic Sulfur and Organic-Matter Contents in Spanish Subbituminous Coals by X-Ray Power Diffraction. *Int. J. Coal Geol.* **1993**, *22*, 279–293. [[CrossRef](#)]
44. Klug, H.P.; Alexander, L.E. *X-Ray Diffraction Procedures: For Polycrystalline and Amorphous Materials*, 2nd ed.; Wiley-Interscience: Cambridge, UK, 1974.

45. Querol, X.; Whateley, M.K.G.; FernandezTuriel, J.L.; Tuncali, E. Geological controls on the mineralogy and geochemistry of the Bepazari lignite, central Anatolia, Turkey. *Int. J. Coal Geol.* **1997**, *33*, 255–271. [[CrossRef](#)]
46. European Council Decision 2003/33/EC. *Off. J. Eur. Communities* **2003**, *16*, 27–49.
47. Querol, X.; Fernandezturiel, J.L.; Lopezsofer, A. Trace-Elements in Coal and Their Behavior during Combustion in a Large Power-Station. *Fuel* **1995**, *74*, 331–343. [[CrossRef](#)]
48. Font, O.; Querol, X.; Izquierdo, M.; Alvarez, E.; Moreno, N.; Diez, S.; Alvarez-Rodriguez, R.; Clemente-Jul, C.; Coca, P.; Garcia-Pena, F. Partitioning of elements in a entrained flow IGCC plant: Influence of selected operational conditions. *Fuel* **2010**, *89*, 3250–3261. [[CrossRef](#)]
49. Zhang, Y.H.; Bai, X.F.; Ding, H.; Wang, Y. The relationship between coal rock characteristics and coal quality and process performance in Junggar coalfield. *Coal Technol.* **2016**, *6*, 1–6. [[CrossRef](#)]
50. Dai, S.F.; Ren, D.Y.; Chou, C.L.; Finkelman, R.B.; Seredin, V.V.; Zhou, Y.P. Geochemistry of trace elements in Chinese coals: A review of abundances, genetic types, impacts on human health, and industrial utilization. *Int. J. Coal Geol.* **2012**, *94*, 3–21. [[CrossRef](#)]
51. Ketris, M.P.; Yudovich, Y.E. Estimations of Clarkes for Carbonaceous biolithes: World averages for trace element contents in black shales and coals. *Int. J. Coal Geol.* **2009**, *78*, 135–148. [[CrossRef](#)]
52. Moreno, N.; Querol, X.; Andres, J.M.; Stanton, K.; Towler, M.; Nugteren, H.; Janssen-Jurkovicova, M.; Jones, R. Physico-chemical characteristics of European pulverized coal combustion fly ashes. *Fuel* **2005**, *84*, 1351–1363. [[CrossRef](#)]
53. Hower, J.C.; Groppo, J.G.; Graham, U.M.; Ward, C.R.; Kostova, I.J.; Maroto-Valer, M.M.; Dai, S.F. Coal-derived unburned carbons in fly ash: A review. *Int. J. Coal Geol.* **2017**, *179*, 11–27. [[CrossRef](#)]
54. ASTM Standard C618-12. *Standard Specification for Coal Fly Ash and Raw or Calcined Natural Pozzolan for Use in Concrete*; ASTM International: West Conshohocken, PA, USA, 2012.
55. Hower, J.C. Petrographic examination of coal-combustion fly ash. *Int. J. Coal Geol.* **2012**, *92*, 90–97. [[CrossRef](#)]
56. Mardon, S.M.; Hower, J.C. Impact of coal properties on coal combustion by-product quality: Examples from a Kentucky power plant. *Int. J. Coal Geol.* **2004**, *59*, 153–169. [[CrossRef](#)]
57. Mastalerz, M.; Hower, J.C.; Drobniak, A.; Mardon, S.M.; Lis, G. From in-situ coal to fly ash: A study of coal mines and power plants from Indiana. *Int. J. Coal Geol.* **2004**, *59*, 171–192. [[CrossRef](#)]
58. Thomas, M.; Jewell, R.; Jones, R. Coal fly ash as a pozzolan. In *Coal Combustion Products (CCP's), Characteristics, Utilization and Beneficiation*; Woodhead Publishing: Sawston, UK, 2017; pp. 121–154.
59. Dai, S.F.; Zhao, L.; Peng, S.P.; Chou, C.L.; Wang, X.B.; Zhang, Y.; Li, D.; Sun, Y.Y. Abundances and distribution of minerals and elements in high-alumina coal fly ash from the Jungar Power Plant, Inner Mongolia, China. *Int. J. Coal Geol.* **2010**, *81*, 320–332. [[CrossRef](#)]
60. Zyrkowski, M.; Neto, R.C.; Santos, L.F.; Witkowski, K. Characterization of fly-ash cenospheres from coal-fired power plant unit. *Fuel* **2016**, *174*, 49–53. [[CrossRef](#)]
61. Ranjbar, N.; Kuenzel, C. Cenospheres: A review. *Fuel* **2017**, *207*, 1–12. [[CrossRef](#)]
62. Goodarzi, F.; Sanei, H. Plerosphere and its role in reduction of emitted fine fly ash particles from pulverized coal-fired power plants. *Fuel* **2009**, *88*, 382–386. [[CrossRef](#)]
63. Dai, S.F.; Zhao, L.; Hower, J.C.; Johnston, M.N.; Song, W.J.; Wang, P.P.; Zhang, S.F. Petrology, Mineralogy, and Chemistry of Size-Fractioned Fly Ash from the Jungar Power Plant, Inner Mongolia, China, with Emphasis on the Distribution of Rare Earth Elements. *Energy Fuels* **2014**, *28*, 1502–1514. [[CrossRef](#)]
64. Hower, J.C.; Qian, D.L.; Briot, N.J.; Henke, K.R.; Hood, M.M.; Taggart, R.K.; Hsu-Kim, H. Rare earth element associations in the Kentucky State University stoker ash. *Int. J. Coal Geol.* **2018**, *189*, 75–82. [[CrossRef](#)]
65. Wagner, N.J.; Matiane, A. Rare earth elements in select Main Karoo Basin (South Africa) coal and coal ash samples. *Int. J. Coal Geol.* **2018**, *196*, 82–92. [[CrossRef](#)]
66. Wang, Z.; Dai, S.F.; Zou, J.H.; Frenck, D.; Graham, I.T. Rare earth elements and yttrium in coal ash from the Luzhou power plant in Sichuan, Southwest China: Concentration, characterization and optimized extraction. *Int. J. Coal Geol.* **2019**, *203*, 1–14. [[CrossRef](#)]

